Specific Transport of Temozolomide Does Not Override DNA Repair-mediated Chemoresistance

Katayan Bahrami [a], Jussi Kärkkäinen [a], Sania Bibi [b], Johanna Huttunen [a], Janne Tampio [a], Ahmed B. Montaser [a], Catherine L. Moody [b], Marko Lehtonen [a], Jarkko Rautio[a], Richard T. Wheelhouse [b], Kristiina M. Huttunen [a,]*

[a] School of Pharmacy, Faculty of Health Sciences, University of Eastern Finland, P.O. Box 1627, FI-70211 Kuopio, Finland

[b] School of Pharmacy, University of Bradford, Bradford, BD7 1DP, UK

* Corresponding author, E-mail: kristiina.huttunen@uef.fi; ORCID: 0000-0002-1175-8517

Abstract

Temozolomide (TMZ) a DNA alkylating agent, is the standard-of-care for brain tumors, such as glioblastoma multiforme (GBM). Although the physicochemical and pharmacokinetic properties of TMZ, such as chemical stability and the ability to cross the blood-brain barrier (BBB), have been questioned, the acquired chemoresistance has been the main limiting factor of long-term clinical use of TMZ. In the present study, an L-type amino acid transporter 1 (LAT1)-utilizing prodrug of TMZ (TMZ-AA, **6**) was prepared and studied for its cellular accumulation and cytotoxic properties in human squamous cell carcinoma, UT-SCC-28 and UT-SCC-42B cells, and TMZ-sensitive human glioma, U-87MG cells that expressed functional LAT1. TMZ-AA **6** accumulated more effectively than TMZ itself into those cancer cells that expressed LAT1 (UT-SCC-42B). However, this did not correlate with decreased viability of treated cells. Indeed, TMZ-AA **6**, similarly to TMZ itself, required adjuvant inhibitor(s) of DNA-repair systems, *O*6-methylguanine-DNA methyl transferase (MGMT) and base excision repair (BER), as well as active DNA mismatch repair (MMR), for maximal growth inhibition. The present study shows that improving the delivery of this widely-used methylating agent is not the main barrier to improved chemotherapy, although utilizing a specific transporter overexpressed at the BBB or glioma cells can have targeting advantages. To obtain a more effective anticancer prodrug, the compound design focus should shift to altering the major DNA alkylation site or inhibiting DNA repair systems.

Keywords: temozolomide (TMZ); L-type amino acid transporter 1 (LAT1); prodrug; chemoresistance; DNA repair

Abbreviations: AIC, 4-amino-5-imidazole-carboxamide; BER, base excision repair system; BBB, blood-brain barrier; BG, *O*6-benzylguanine; GBM, glioblastoma multiforme; LAT1, L-type amino acid transporter 1; MGMT, *O*6-methylguanine-DNA methyl transferase; MMR, mismatch repair system; MTIC, 5-(3-methyltriazen-1-yl)-imidazole-4-carboxamide; *N*3-MeA, *N*3-methyladenine; *N*7-MeG, *N*7-methylguanine; *O*6-MeG, *O*6-methylguanine; MX, methoxyamine; SLC, several solute carriers; TMZ, temozolomide; TMZ-AA, temozolomide amino acid prodrug

1 Introduction

Primary malignant brain tumors and metastatic secondary brain tumors are very challenging to treat (1-3). Therefore, the prognoses of these devastating diseases are often very poor. In particular, glioblastoma multiforme (GBM), IV-grade malignant astrocytoma, has extremely low 5- and 10-year survival rates (ca. 5% and 2%) from the time of diagnosis (4). Today, GBM and other brain tumors are treated by surgery, radiotherapy, chemotherapy, or a combination of these depending on the tumor type and its location. However, the challenge to most chemotherapy arises from the blood-brain barrier (BBB) preventing many drugs from penetrating into the brain and subsequently into the cancerous cells (5-8). Moreover, intrinsic and/or acquired (adapted) chemoresistance diminishes the therapeutic success of anti-cancer agents intended to treat brain tumors (9).

Temozolomide (TMZ), an imidazotetrazine, is an oral alkylating agent that has become a first-line treatment for GBM, since its approval in 2005 by the US Food and Drug Administration (FDA), and a blockbuster drug since 2010 (10, 11). TMZ undergoes hydrolysis in neutral and slightly basic conditions to yield 5-(3-methyltriazen-1-yl)-imidazole-4-carboxamide (MTIC) and this then fragments further to 4-amino-5-imidazole-carboxamide (AIC) and highly reactive methyl diazonium ion (**Figure 1**)(12). Methyl diazonium methylates DNA guanine residues at *N*7- and *O*6-positions and adenine residues at *N*3-positions. Although the 6-position of guanine (*O*6-MeG) in DNA is the least frequently methylated site (ca. 5-8%), it confers the most genotoxic effect of TMZ. Mispairing of *O*6-MeG with thymine instead of cytosine during DNA replication is the key step in the pathway to DNA strandbreaks (13). In this step, mismatch repair (MMR) enzymes attempt the restoration of genomic integrity by identifying, excising, and replacing the mispaired nucleotide bases. However, the removal of mispaired thymine initiates repetitive cycles of reinsertion and excision of thymine. This, in turn, results in the accumulation of multiple single- and double-strand breaks that lead to cell cycle arrest, and ultimately to apoptosis.

Although TMZ is easily absorbed (nearly 100% oral bioavailability) and crosses the BBB relatively effectively (ca. 10-20%), it suffers from a short hydrolytic half-life (less than 2 h at pH 7.4) (10). Moreover, intrinsic and acquired chemoresistance compromise TMZ chemotherapy. These resistance mechanisms are to some extent characterized at the genetic level, however, more focus should also be paid to epigenetics, transcriptomics, and proteomics of TMZ chemoresistance (14). The most significant TMZ-resistance mechanism, that

determines first-line tumour response, is *O*6-methylguanine-DNA methyl transferase (MGMT), a repair protein that restores wild-type guanine from TMZ-induced *O*6-MeG adducts and so maintains the genomic function (**Figure 1**) (9, 15). In contrast, the DNA MMR system, which accounts for the cytotoxic effects of TMZ in normal conditions, has been recognized to malfunction in some cancer cells, and thus its lack of function serves as a second chemoresistance mechanism (9, 14, 15). A third resistance mechanism is base excision repair (BER) that resolves *N*7-methylguanine (*N*7-MeG) and *N*3-methyladenine (*N*3-MeA) aducts (14, 16). Although these are the major DNA methylation products of TMZ (> 79%), effective repair means they induce only a little genotoxicity compared with *O*6-MeG (**Figure 1**). Although attractive in preclinical studies, combinations of TMZ with DNA damage response (DDR) inhibitors (*e.g.*, targeting MGMT, poly ADP ribose polymerase (PARP), or ATM/ATR kinases) have failed to translate to clinical benefit due to increased systemic toxicity. To solve the problem of the low hydrolytic stability of TMZ, novel analogs of TMZ as well as delivery methods, such as nanocarriers, have been proposed to improve the therapeutic potential of TMZ itself (17-20).

Several solute carriers (SLCs) are overexpressed in different cancer cell types, including the L-type amino acid transporter 1 (LAT1) (21, 22). As we have shown with various compounds, attaching an amino acid residue to an active parent drug can convert it into a LAT1-substrate that can be transported into cancer cells (23-26). Therefore, the aim of the present study was to develop a LAT1-utilizing derivative of TMZ and explore 1) whether its specific cellular uptake could be increased by LAT1-utilization and 2) whether this can affect the cell viability of human squamous cell carcinoma from the oral cavity and larynx (UT-SCC-28 and UT-SCC-42B cells) and TMZ-sensitive human glioma U-87MG cells.

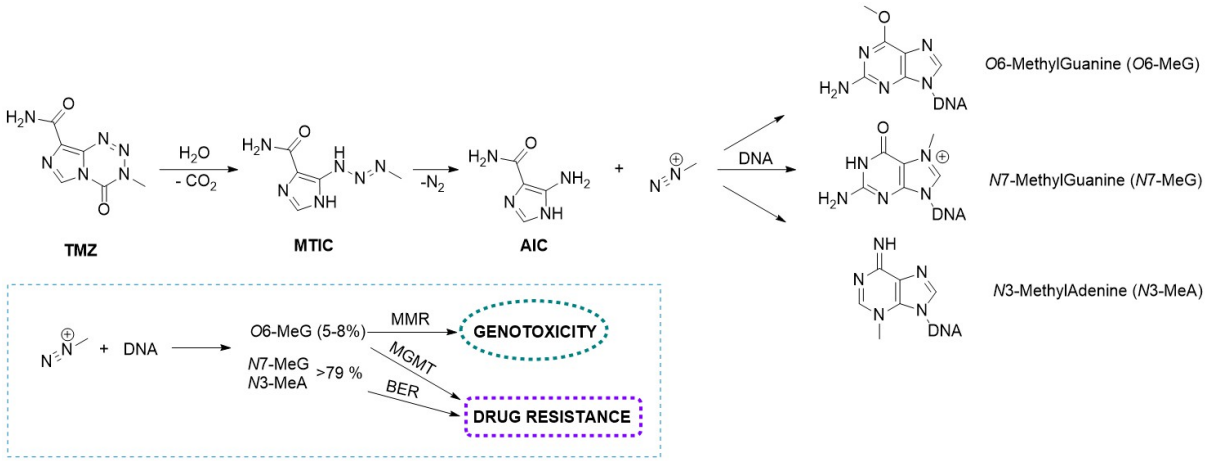

Figure 1. Activation and chemoresistance mechanisms of temozolomide (TMZ). Reactive methyldiazonium ion, generated from TMZ via 5-(3-methyltriazen-1-yl)-imidazole-4-carboxamide (MTIC) reacts with DNA guanine residues at *N*7- and *O*6-positions (to generate *O*6-MeG and *N*7-MeG) and adenine residues at *N*3-positions (to give *N*3-MeA). The activity of *O*6-MeG is dependent on the futile cycles of the mismatch repair (MMR) system, while *O*6-methylguanine-DNA methyl transferase (MGMT) and base excision repair (BER) are the main repair pathways of *O*6-MeG, *N*7-MeG, and *N*3-MeA and are thus the main mechanisms of chemoresistance to TMZ.

2 Materials and Methods

2.1 General Synthetic Materials and Methods

All reactions were performed with reagents obtained from Sigma-Aldrich (Poole, UK), Thermofisher (Loughborough, UK) or Merck (Darmstadt, Germany). Reactions were monitored by thin-layer chromatography using aluminum sheets coated with silica gel 60 F_{245} (0.24 mm) with suitable visualization. Purifications by flash chromatography were performed on silica gel 60 (0.063-0.200 mm mesh). ^{1}H and ^{13}C nuclear magnetic resonance (NMR) spectra were recorded on a Bruker-spectrospin AC400 spectrometer observing ^{1}H at 400.13 MHz and ^{13}C at 100.62 MHz using solvent ^{2}H as a reference. Infrared data were obtained using a Perkin Elmer (Paragon 1000) FT-IR Spectrophotometer. Mass spectra were obtained from the Analytical Centre at the University of Bradford using a Micromass Quattro Ultima mass spectrometer (MS). Elemental analyses were obtained from the Advanced Chemical and Material Analysis Unit at the University of Newcastle upon Tyne, UK. ^{1}H and ^{13}C NMR spectra, MS scans and IR spectrum of the final compound (**6**) can be found in the Supporting Information (**Figures S1-4**).

*2.2 (S)-4'-(3-nitrobenzyl)-5'-oxospiro[bicyclo[3.3.1]nonane-9,2'-[1,3,2]oxazaborolidin]-3'-ium-11-uide (**1**)ref 36*

9λ^{4}-Boraspiro[bicyclo[3.3.1]nonane-9,2'-[1,3,2]oxazaborolidin]-5'-one (9-BBN; 956 mg, 3.91 mmol) in MeOH (20 mL) under N_2 was heated to reflux. 3-Nitrophenylalanine (748 mg, 3.46 mmol) was added in one portion and the reaction mixture was maintained at reflux for 3 h. The resulting solid was filtered, washed with MeOH (50 mL) and dried *in vacuo* to give a white powder as compound **1** (984 mg, 2.98 mmol, 84%). ^{1}H NMR (400 MHz, DMSO-d_6): δH 8.80 (1H, br s, *H*-2), 8.13, (1H, dd, *J* = 8.0, 2.0 HZ, *H*-6), 7.83 (1H, d, *J* = 7.5 Hz, *H*-4), 7.63 (1H, app. t, *J* = 8.0 Hz, *H*-5), 6.38 (1H, dd, *J* = 11.0, 7.5 Hz, N*H*H), 6.01 (1H, dd, *J* = 11.0, 10.0 Hz, NH*H*), 4.00–3.92 (1H, m, NC*H*), 3.34 (1H, dd, *J* = 14.5, 4.5 Hz, C*H*H), 3.05 (1H, dd, *J* = 14.5, 9.5 Hz, CH*H*), 1.84–1.31 (12H, m, 6xC$H_2$of BBN), 0.48 (2H, br s, 2xBCH); ^{13}C NMR (100 MHz, DMSO-d_6): δC 172.6 (*C*=), 147.6 (q), 139.7 (q), 136.3 (*C*-4/6), 129.6 (*C*-5), 124.4 (*C*-2), 121.5 (*C*-4/6), 55.4 (*C*H), 35.4 (*C*H_2), 31.1, 31.1, 30.6, 30.4, 24.1 (*C*-B), 23.8 (*C*-B). LRMS (API+) m/z 331.3 $[M+H]^+$. IR (KBr): υ_{max} 3320, 3226, 2936, 2891, 2860, 2840, 1726, 1513 cm^{-1}.

*2.3 (S)-4'-(3-Aminobenzyl)-5'-oxospiro[bicyclo[3.3.1]nonane-9,2'-[1,3,2]oxazaborolidin]-3'-ium-11-uide (**2**)ref 36*

(*S*)-4'-(3-Nitrobenzyl)-5'-oxospiro[bicyclo[3.3.1]nonane-9,2'-[1,3,2]oxazaborolidin]-3'-ium-11-uide **1** (290 mg, 0.63 mmol), 10% Pd/C (46 mg) and ethyl acetate (25 mL) were stirred under an atmosphere of hydrogen (balloon) at RT for 2 h. The reaction mixture was transferred to a centrifuge tube and spun at 3500 rpm for 10 min before filtering through paper and concentrating *in vacuo* to give a viscous colourless oil as compound **2** (189 mg, quant.). ^{1}H NMR (400 MHz, MeOD-d_3): δH 7.09 (1H, dd, *J* = 7.5, 8.5 Hz, Ar-*H*), 6.67–6.60 (3H, m, Ar-*H*), 4.90–4.82 (2H, br, NH_2), 3.98–3.92 (1H, m, C*H*), 3.17 (1H, dd, *J* = 5.0, 14.5 Hz, C*H*H), 2.97 (1H, dd, *J* = 8.0, 14.5 Hz, CH*H*), 1.90–1.35 (12H, m, 6xCH_2 of BBN), 0.55 (1H, br s, BC*H*), 0.29 (1H, br s, BC*H*); ^{13}C NMR (100 MHz, MeOD-d_3): δC 176.5 (*C*=O), 149.7 (q), 138.1 (q), 130.9, 119.8, 117.1, 115.6, 57.6 (α-*C*), 37.4 (β-*C*), 32.6, 32.5, 32.4, 32.2, 25.7 (*C*-B), 25.2 (C-B). LRMS (API+) m/z 301.1 $[M+H]^+$

*2.4 3-Methyl-4-oxo-3,4-dihydroimidazo[5,1-d][1,2,3,5]tetrazine-8-carboxylic acid (**3**)ref 37*

To TMZ (1 g, 5.15 mmol) in conc. H_2SO_4 (12 mL) in an ice bath was added dropwise a solution of $NaNO_2$ (3.5 eq, 1.25 g, 18.1 mmol), maintaining T below 20 °C (mostly < 10 °C) for ca. 1 h. The reaction mixture was allowed to warm to RT and stirred for 4 h. The mixture was then poured into ice (150 mL) and stirred for 5 min. The precipitate was filtered, washed with H_2O and a small quantity of cold acetone to yield compound **3**. ^{1}H NMR (400 MHz, DMSO-d_6): δH 13.29 (1H, br s, O*H*), 8.80 (1H, s, C*H*), 3.87 (3H, s, CH_3). IR (KBr): υ_{max} 3515, 3451, 3084, 1766, 1690 cm^{-1}.

*2.5 3-Methyl-4-oxo-3,4-dihydroimidazo[5,1-d][1,2,3,5]tetrazine-8-carbonyl chloride (**4**) ref 37*

3-Methyl-4-oxo-3,4-dihydroimidazo[5,1-d][1,2,3,5]tetrazine-8-carboxylic acid **3** (195 mg, 1.0 mmol) and DMF (0.1 mL) in thionyl chloride (1.8 mL) were stirred at 80 °C for 2 h. The reaction mixture was concentrated *in vacuo* and azeotroped with PhMe to give the title compound **4** as a yellow solid (quant.) ^{1}H NMR (400 MHz, DMSO-d_6): δH 8.81 (1H, s, C*H*), 3.88 (3H, s, CH_3).

*2.6 (S)-4'-(3-(3-Methyl-4-oxo-3,4-dihydroimidazo[5,1-d][1,2,3,5]tetrazine-8-carboxamido)benzyl)-5'-oxospiro[bicyclo[3.3.1]nonane-9,2'-[1,3,2]oxazaborolidin]-3'-ium-11-uide (**5**)*

To 3-methyl-4-oxo-3,4-dihydroimidazo[5,1-d][1,2,3,5]tetrazine-8-carbonyl chloride **4** (0.50 mmol) in $CHCl_3$ was added a solution of (*S*)-4'-(3-aminobenzyl)-5'-

oxospiro[bicyclo[3.3.1]nonane-9,2'-[1,3,2]oxazaborolidin]-3'-ium-11-uide **2** (0.60 mmol) in $CHCl_3$ (5 mL) followed by addition of Et_3N (152 μL, 1.1 mmol). The reaction mixture was stirred at RT overnight. The mixture was then concentrated, triturated with H_2O and filtered to give the title compound **5** as a yellow solid, 155 mg (65% from 3-methyl-4-oxo-3,4-dihydroimidazo[5,1-d][1,2,3,5]tetrazine-8-carboxylic acid **3**). ^{1}H NMR (400 MHz, DMSO-d_6): δH 10.26 (1H, s, N*H*), 8.96 (1H, s, C*H*), 7.84 (1H, br s, *H*-2), 7.77 (1H, d, *J* = 8.0 Hz, *H*-6), 7.31 (1H, t, *J* = 8.0 Hz, *H*-5), 7.12 (1H, d, *J* = 8.0 Hz, *H*-4), 6.51 (1H, dd, *J* = 7.5, 11.0 Hz, BN*H*), 5.83 (1H, dd, *J* = 9.0, 11.0 Hz, BN*H*), 3.90 (3H, s, CH_3), 3.84 (1H, m, C*H*), 3.19 (1H, dd, *J* = 5.0, 14.5 Hz, C*H*H), 2.98 (1H, dd, *J* = 8.5, 14.5 Hz, CH*H*), 1.85–1.30 (12H, m, 6xCH_2 of BBN), 0.49 (2H, br s, 2xBC*H*); ^{13}C NMR (100 MHz, DMSO-d_6): δC 173.2 (*C*=O), 158.3 (*C*=O), 139.2 (*C*=O), 138.3 (q-*C*), 138.0 (q-*C*), 135.2 (q-*C*), 130.1 (q-*C*), 128.7 (*C*-5), 128.6 (*C*H), 125.0 (*C*-4), 121.2 (*C*-2), 118.6 (*C*-6), 55.8 (*C*HNH$_2$), 36.3 (*C*H$_3$), 36.2 (*C*H$_2$), 31.4, 31.2, 30.7, 30.6, 24.3 (*C*-B), 23.9 (*C*-B). LRMS (ESI+) m/z 500.3 $[M+Na]^+$. IR (KBr): υ_{max} 3125, 2920, 2843, 1743, 1702, 1611, 1595, 1570, 1536, 1489 cm^{-1}.

*2.7 (S)-1-Carboxy-2-(3-(3-methyl-4-oxo-3,4-dihydroimidazo[5,1-d][1,2,3,5]tetrazine-8-carboxamido)phenyl)ethanaminium bromide (**6**)*

(*S*)-4'-(3-(3-Methyl-4-oxo-3,4-dihydroimidazo[5,1-d][1,2,3,5]tetrazine-8-carboxamido)benzyl)-5'-oxospiro[bicyclo[3.3.1]nonane-9,2'-[1,3,2]oxazaborolidin]-3'-ium-11-uide **5** (86 mg, 0.18 mmol) in acetonitrile (8 mL) was briefly sonicated. HBr (0.5 mL) was added dropwise and the reaction mixture stirred at RT for 24 h. Further MeCN (5 mL) was added and the suspension was filtered and washed with MeCN under N_2 to give a pale yellow solid **6** (63 mg, 0.14 mmol, 77%). ^{1}H NMR (400 MHz, MeOD-d_3): δH 8.67 (1H, s, C*H*), 7.87 (1H, s, *H*-2), 7.60 (1H, d, *J* = 8.0 Hz, *H*-6), 7.39 (1H, t, *J* = 8.0 Hz, *H*-5), 7.14 (1H, d, *J* = 8.0 Hz, *H*-4), 4.33 (1H, dd, *J* = 8.0, 5.0 Hz, C*H*), 4.01 (3H, s, CH_3), 3.39 (1H, dd, *J* = 14.5, 5.0 Hz, C*H*H), 3.19 (1H, dd, *J* = 14.5, 8.0 Hz, CH*H*); ^{13}C NMR (100 MHz, MeOD-d_3): δC 171.2 (C=O), 160.6 (C=O), 140.4 (C=O), 139.7 (q-*C*), 136.8 (q-*C*), 136.6 (q-*C*), 131.3 (q-*C*), 130.8 (*C*-5), 129.8 (*C*H), 127.0 (*C*-4), 122.9 (*C*-2), 121.3 (*C*-6), 55.2 (*C*H), 37.4 (*C*H$_3$), 37.1 (*C*H$_2$). LRMS (ESI+) m/z 358.1 $[M+H]^+$, 380.1 $[M+Na]^+$. Anal. Calcd for ($C_{15}H_{16}BrN_7O_4 \cdot 0.75H_2O$): C, 39.88%; H, 3.90%; N, 21.70%; Found: C, 39.81%; H, 3.91%; N, 21.96%.

2.8 Stability of Studied Compounds in Buffer Solution at pH 7.4

The chemical stabilities of the novel compound **6** and TMZ in buffer solution at pH 7.4 were determined by incubating 10 mM stock solution of studied compounds (DMSO) in 50 mM Tris

buffer (pH 7.4) at 37 °C (the final concentrations of compounds were 100 µM and the DMSO concentration 2%). The mixtures were incubated for 24 h and the samples (100 µL) were withdrawn at appropriate intervals. The chemical reaction was quenched by adding ice-cold acetonitrile (100 µL) containing 0.1% of formic acid. The samples were centrifuged for 5 min at 12 000 x *g* and the supernatants were analyzed by the liquid chromatography-mass spectrometry (LC-MS) method described below. The pseudo-first-order half-lives ($t_{½}$) for the rates of bioconversion of the compounds were calculated from the slope of the linear portion of the logarithm of the remaining compound concentration versus time plot. Similarly, the stability in 0.1% formic acid (pH 3) was studied at room temperature (RT) for 4 h.

2.9 Liquid Chromatography Mass Spectrometric Analysis (LC-MS)

The amounts of TMZ and its LAT1-utilizing derivative **6** (TMZ-AA) were quantified by an LC-MS method with an Agilent 1200 Series Rapid Resolution LC System together with an Agilent 6410 Triple Quadrupole Mass Spectrometer (Agilent Technologies, Santa Clara, CA, USA). Diclofenac was used as an internal standard. First, the studied compounds were separated using a reverse-phase column (Zobrax Eclipse XDB-C18, 4.6 mm × 50 mm, 1.8 µm; Agilent Technologies, Santa Clara, CA, USA) and a mobile phase of 0.1% formic acid in water (A) and acetonitrile (B). The injected sample volume was 5 µL, and the column temperature was 40 °C. The mobile phase flow rate was 0.5 mL/min with the following gradient: 0−4 min, 2% B → 35%; 4−4.5 min, 35% B → 95%; 4.5−7.5 min, 95% B; 7.5−8 min, 95% B → 2%; 8−10.5 min, 2% B.

For the mass spectrometric analysis, an electrospray ionization source was used in positive mode (ESI+) with the following conditions: the drying gas (nitrogen) temperature was 300 °C with a gas flow rate of 8 L/min, the nebulizer pressure was 40 psi, and the capillary voltage was 3.5 kV. The analyte detection was performed using multiple reaction monitoring with the transitions 195→138 for the TMZ, 358.1→312.1 and 358.1→210 for the TMZ-AA, and 296.1→250 for the diclofenac. The fragmentor voltages for TMZ, TMZ-AA, and diclofenac were 80 V, 140 V, and 100 V, respectively. The collision energies for product ions of TMZ, TMZ-AA, and diclofenac were 2 V, 8 V, 12 V, and 10 V, respectively. The data acquisition software was Agilent MassHunter Workstation software (version B.03.01), whereas Quantitative Analysis (B.09.00) software was used for data processing and analysis. The method was validated for the selectivity, linearity, accuracy, and precision (deviation ≤ 20% of

the nominal concentrations) over the calibration range of 0.005–2.5 nmol/mL for TMZ, and 0.0025–2.5 nmol/mL for TMZ-AA.

2.10 General Analytical Materials and Methods

All reagents and solvents used in analytical studies were commercial and high purity of analytical grade or ultra-gradient HPLC-grade purchased from MilliporeSigma (St. Louis, MO, USA), ThermoFisher Scientific (Waltham, MA, USA), J.T. Baker (Deventer, The Netherlands), Riedel-de Haën (Seelze, Germany), EuroClone S.p.A. (Pero, Italy), or Promega Biotech AB (Nacka, Sweden). Water was purified using a Milli-Q Gradient system (Millipore, Milford, MA, USA).

Human glioma U-87MG cells were purchased from the American Type Culture Collection (ATCC, Manassas, VA, USA) and human and squamous cell carcinoma cells, UT-SCC-28 and UT-SCC-42B, were kindly provided by Professor Reidar Grenman at the Department of Otorhinolaryngology, University of Turku and Turku University Hospital, Finland. U-87MG cells were cultured in Dulbecco's Modified Eagle Medium (DMEM) supplemented with L-glutamine (2.0 mM), heat-inactivated fetal bovine serum (10%), penicillin (50 U/mL)-streptomycin (50 µg/mL) solution. UT-SCC-28 and UT-SCC-42B cells were cultured in Dulbecco's Modified Eagle Medium (DMEM; Lonza™ BioWhittaker™, ThermoFisher Scientific, Valais, Switzerland) supplemented with L-glutamine (2.0 mM; ThermoFisher Scientific, Valais, Switzerland), heat-inactivated fetal bovine serum (10%; Gibco, ThermoFisher Scientific, Waltham, MA, USA), penicillin (100 U/mL)-streptomycin (100 µg/mL) solution (Lonza™ BioWhittaker™, ThermoFisher Scientific, Valais, Switzerland) and nonessential amino acids (0.1mM) solution (Lonza™ BioWhittaker™, ThermoFisher Scientific, Valais, Switzerland). The cells were used for the experiments one day after seeding. All studies were carried out as three biological replicates from the same cell passage. The function of LAT1 was followed between the used cell passages with a LAT1 probe substrate, [^{14}C]-L-leucine (0.76 µM), and noticed to be un-altered.

2.11 Expression of LAT1 in Selected Cell Lines

The absolute expressions of L-type amino acid transporter 1 (LAT1) light chain, CD98 heavy chain (4F2hc), and glucose transporter 1 (GLUT1) together with sodium-potassium adenosine triphosphatase (Na^+/K^+-ATPase) were quantified from the plasma membrane fractions of human glioma U-87MG, and squamous cell carcinomas UT-SCC-28 and UT-SCC-42B cells

as well as human breast cancer (MCF-7) as a control, by the LC-MS/MS method following a multiplexed multiple reaction monitoring (MRM) analysis mode according to the protocol described previously (27) with minor modifications (28-30). The plasma membrane fractions were isolated from three distinct sets of cell culture plates (biological replicates) by using Membrane Protein Extraction Kit (BioVision Incorporated, Milpitas, CA, USA) according to the manufacturer's instructions. The protein content for each fraction was measured by Pierce™ BCA Protein Assay Kit (Thermo Fisher Scientific, Inc., Waltham, MA, USA) and a total amount of 50 µg proteins from each fraction were denatured, reduced, and alkylated. Finally, the peptides in the precipitated protein pellet were digested with LysC (1/100, w/w) and 0.05% ProteaseMax for 3 h at room temperature. The samples were spiked with 10 µL (30 fmol) of the labeled peptides for absolute quantification (**Table 3**) and further digested with TPCK-Trypsin (1/100, w/w; Promega Biotech AB, Nacka, Sweden) for 18 h at 37 °C, followed by acidification. The digested peptides in each sample were analyzed using an ultra-performance liquid chromatography system coupled with a triple quadrupole mass spectrometer with a heated electrospray ionization source in the positive mode (UPLC 1290 and MSD 6495, Agilent Technologies, Santa Clara, CA, USA). A total amount of 20 µL of the digested peptides (10 µg) was separated using AdvanceBio Peptide Map 2.1 × 250 mm, 2.7 µm column (Agilent Technologies, Santa Clara, CA, USA), eluting with of 0.1% formic acid in water (A) and acetonitrile (B) with a constant flow rate of 0.3 mL/min and a gradient of 2-7% B for 2 min, followed by 7-30% B for 48 min, 30-45% B for 3 min, and 45-80% B for 2.5 min before re-equilibrating the column again for 4.5 min. The proteins were quantified based on the ratio between the light and heavy standard peptides, as described previously (**Table 3**) (29). Data were acquired using Agilent MassHunter Workstation Acquisition (Agilent Technologies, Data Acquisition for Triple Quadrupole, version B.03.01) and processed by using Skyline software (version 20.1). The results were compared with a housekeeping protein Na^+/K^+ATPase and expressed as fmol/µg of the total amount of protein in the samples.

Table 3. SRM/MRM transitions for absolute quantitative proteomics (31, 32).

Protein	Gene	Peptide	Type	Retention time (min)	Precursor ion Q1	Product ions		
						Q3-1	Q3-2	Q3-3
Na^+K^+ATPase	*ATP1A1-3*	AAVPDAVGK	St	10.3	414.23	685.39	586.32	489.27
		AAVPDAVG**K***	SIS	10.3	418.24	693.40	594.33	497.28
LAT1	*SLC7A5*	VQDAFAAAK	St	12.7	460.75	693.36	578.33	821.42
		VQDAFAA***AK	SIS	12.7	462.75	697.36	582.34	825.42
4F2hc	*SLC3A2*	VAGSPGWVR	St	18.0	464.75	711.38	624.35	527.30
		VAGSPGWVR*	SIS	18.0	469.76	894.43	779.4	650.36
GLUT1	*SLC2A1*	TFDEIASGFR	St	29.2	571.78	894.43	537.28	650.36
		TFDEI**A***SGFR	SIS	29.2	573.78	898.44	541.29	654.37

2.12 Function of LAT1 in Selected Cell Lines

The cells (passages 10-40) were seeded at the density of 1×10^5 cells/well onto 24-well plates. After removal of the culture medium, human glioma U-87MG, and squamous cell carcinomas UT-SCC-28 and UT-SCC-42B cells were carefully washed with pre-warmed HBSS (Hank's balanced salt solution) containing 125.0 mM NaCl (or choline chloride in Na^+ free conditions), 4.8 mM KCl, 1.2 mM $MgSO_4$, 1.2 mM KH_2PO_4, 1.3 mM $CaCl_2$, 5.6 mM glucose, and 25.0 mM 4-(2-hydroxyethyl)piperazine-1-ethanesulfonic acid (HEPES) with pH adjusted to 7.4. The cells were pre-incubated with pre-warmed HBSS (500 µL) at 37 °C for 10 min before adding L-leucine in HBSS (250 µL). The functionality of LAT1 in different cells was studied at 37 °C for 10 min with the uptake buffer (250 µL) consisting of 1-500 µM of L-leucine containing 0.76 µM of [^{14}C]-L-leucine (PerkinElmer, Waltham, MA, USA) (2 µCi). After incubation, the uptake was stopped by adding ice-cold HBSS (500 µL), and the cells were washed twice with ice-cold HBSS (2 x 500 µL). The cells were then lysed with NaOH (0.1 M; 500 µL) for 60 min, and the lysate was mixed with Emulsifier safe cocktail (3.5 mL; Ultima Gold, PerkinElmer, Waltham, MA, USA). The radioactivity in the cells was measured by liquid scintillation counting (MicroBeta^2 counter, PerkinElmer Waltham, MA, USA). The concentrations of [^{14}C]-L-leucine were calculated from the spiked standard curve and normalized with the protein concentrations. The LAT1-mediated uptake was confirmed by incubating 0.38 and 0.76 µM [^{14}C]-L-leucine in the presence of LAT1-selective inhibitor (100 µM)(33).

2.13 Transporter-Mediated Uptake of Compounds into Cells

Cellular uptake of temozolomide (TMZ) and its LAT1-utilizing derivative **6** (TMZ-AA) were then studied with human glioma U-87MG, and squamous cell carcinomas UT-SCC-28 and UT-SCC-42B cells by adding compounds at the test concentration (1-200 μM) in pre-warmed HBSS buffer (250 μL) on the cell layer in 24-well plates (1×10^5 cells/well) and incubating the cells at 37 °C for 30 min (uptake was linear with all compounds up to 30 min). Subsequently, the cells were washed three times with ice-cold HBSS and lysed with 1% perchloric acid (250 μL) for 60 min. For the compound quantitation, the samples were precipitated by diluting cell lysates 1:4 (v:v) with ACN containing 200 nM of internal standard (diclofenac). The diluted samples were centrifuged (10 min at 12 000 x *g*) and analyzed by the LC-MS/MS methods described above. The analyte concentrations in cell lysates were calculated from the standard curve that was prepared by spiking known concentrations of compounds to H_2O:ACN (1:4, 0.1% FA) used to lyse the cells and treat the samples, and the results were normalized to protein concentration. The protein concentrations on each plate were determined as a mean of three lysis samples by Bio-Rad Protein Assay, based on the Bradford dye-binding method, using BSA as a standard protein and measuring the absorbance (595 nm) by a multiplate reader (EnVision, Perkin Elmer, Inc., Waltham, MA, USA).

The competitive uptake of TMZ-AA **6** (50 μM) in the presence of selective LAT1-inhibitor (100 μM)(33) was carried out as described above. The cells were pre-incubated with the inhibitor for 10 min and the incubation mixture was removed before adding the studied compound and inhibitor to the cells. The competitive uptake (30 min) in the presence of inhibitor was then carried out as the normal uptake described above. The concentrations of studied compounds were analyzed by the LC-MS/MS method and calculated from the spiked standard curve and normalized with the protein concentrations.

2.14 Cellular Viability in the Presence of Studied Compounds

The viabilities of human glioma U-87MG, and squamous cell carcinomas UT-SCC-28 and UT-SCC-42B cells were determined in the presence of TMZ, TMZ-AA **6**, *O*6-benzylguanine (BG) or methoxyamine (MX), or combinations of BG (100 μM) or MX (100 μM) and TMZ or TMZ-AA (5-200 μM), or BG + MX + TMZ or TMZ-AA (100 + 100 + 5-200 μM) for 72 h. The cells were seeded at the density of 10 000 per well on 96-well plates and maintained for 24 h to obtain over 70% confluency, after which the cells were treated with the above-mentioned compounds or their combinations (37º C, 5% CO_2). After incubation (24, 48, and 72 h), the

cell viability was determined by resazurin cell proliferation kit (Sigma, St. Louis, MO, USA), which is directly proportional to aerobic respiration and cellular metabolism of cells. The samples were measured fluorometrically by monitoring the increase in fluorescence at 590 nm using an excitation wavelength of 544 nm in a Hidex Sense microplate reader (Hidex Oy, Turku, Finland). The measured cell viability was confirmed by visualizing the wells directly by microscopy. Control samples with pure medium and medium containing the solvent (DMSO, 2%) were performed to obtain 100% viability and to follow the effects of solvent on cells. The results were expressed as a percentage of the control samples treated with pure medium (representing 100% viability).

2.15 Data analysis

Statistical analyses were performed using GraphPad Prism v. 9.5.0 (730) software (GraphPad Software, San Diego, CA, USA). Statistical differences between groups were tested using one-way ANOVA, followed by a two-tailed Dunnett's or Tukey's test and presented as * $P < 0.05$, ** $P < 0.01$, *** $P < 0.001$, **** $P < 0.0001$.

3 Results

3.1 Design and Synthesis of LAT1-Utilizing Derivative of TMZ

Based on our previous findings, the LAT1-utilizing derivative of TMZ was designed by attaching L-phenylalanine from its *meta*-position in relation to the amino acid residue, to TMZ (24, 34, 35). Derivatization of TMZ from its amide moiety has shown a broad range of activity in different cell lines and thus, this kind of derivatization is well-tolerated and does not affect the release of methyl diazonium ion from TMZ analogs (10). TMZ amino acid derivative (TMZ-AA, **6**) was obtained in good yields using BBN (9-borobicyclononane) as an amino acid protecting group (**Scheme 1**), while the attempts to prepare compound **6** with *t*-Boc protecting group were not successful. The amino acid derivate **2** was prepared as previously described (36) and TMZ was converted to its corresponding acid chloride **4** by the literature procedure (37). The coupling of TMZ acid chloride **4** with the amino acid **2 also** followed a published procedure (34), giving the TMZ-AA **6** as final product in high purity. Due to the attached amino acid moiety, the new TMZ derivative **6** (TMZ-AA) had increased molecular weight, clogP, and cPSA values compared with TMZ itself (**Table 1**). However, the stability of the novel compound in 50 mM Tris buffer solution at pH 7.4 (+37 °C) was slightly decreased (ca. 3 h) in comparison with TMZ (ca. 3.5 h) while there was no change in stability in acidic conditions between the compounds during 4 h incubation (98-99% stable; **Table 1**).

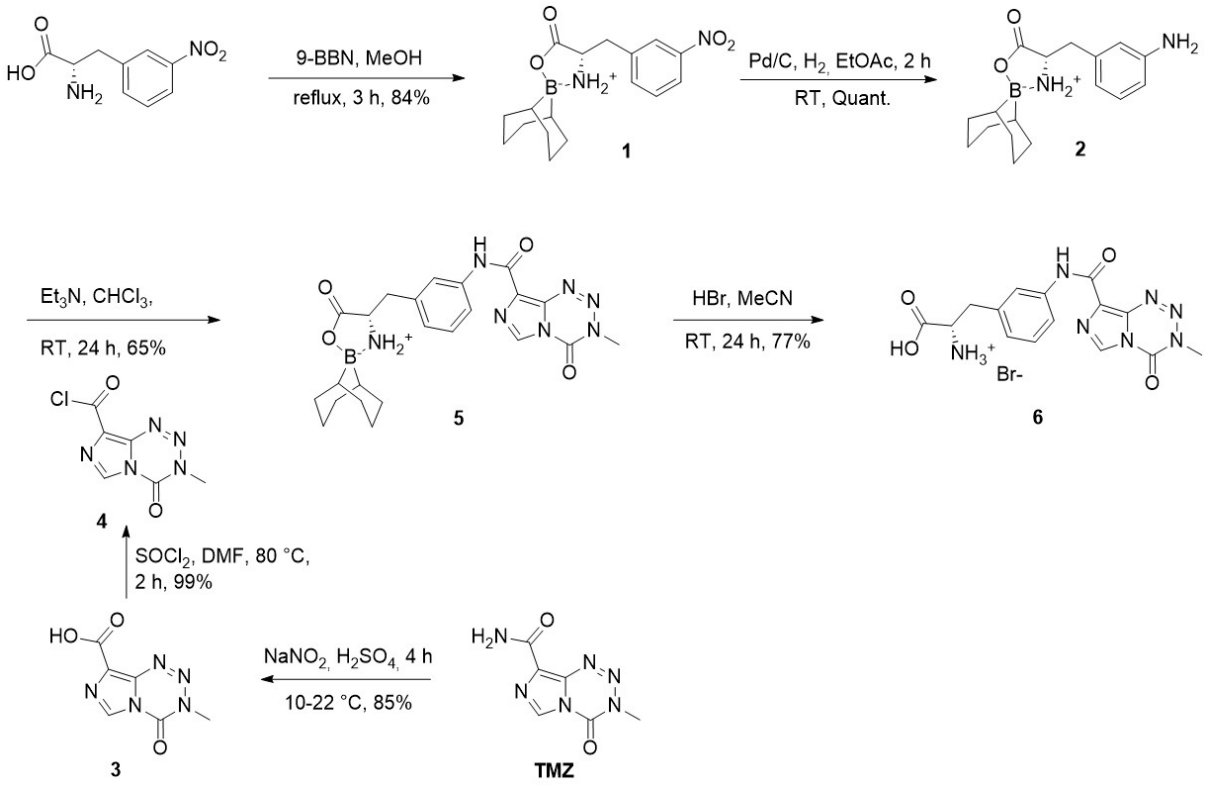

Scheme 1. Synthetic route for the preparation of TMZ-AA (**6**).

Table 1. Physicochemical properties of temozolomide (TMZ) and its LAT1-utilizing derivative TMZ-AA **6** estimated with ChemDraw Professional (PerkinElmer Informatics, Inc. v.20.1.1.125) and their stabilities in buffer solution at pH 7.4 (+37 °C), 0.1 M NaOH pH 8 (RT), and 0.1% formic acid (FA) pH 3 (RT), expressed as half-life ($t_{½}$, min, mean ± SD, n=3).

Properties	**TMZ**	**TMZ-AA**
Mw. (g/mol)	194.15	357.33
cLogP	-0.81	-2.41
cPSA	103.72	153.05
Half-life ($t_{½}$) in 50 mM Tris buffer (pH 7.4, +37 °C) (min)	210 ± 8	181 ± 6
Stability in 0.1% FA (%) (pH 3, RT)	99 ± 1	98 ± 1

3.2 Expression and Function of LAT1 in Selected Cell Lines

The expression of the studied transporter, LAT1, on the plasma membrane of selected cancer cells (human squamous cell carcinoma (UT-SCC-28 and UT-SCC-42B) and human glioma (U-87MG)) was quantified with a targeted proteomic approach using liquid chromatography-mass spectrometric (LC-MS/MS) methods. The expression levels of the light chain (LAT1) and the heavy chain (4F2hc) of the heterodimeric LAT1 complex as well as a generally expressed glucose transporter 1 (GLUT1) were normalized with a housekeeping plasma membrane protein (sodium-potassium adenosine triphosphatase (Na^+/K^+ATPase)). For comparison, the expression of transporters in the human estrogen receptor-positive breast adenocarcinoma cell line, MCF-7, was used, since this cell line has been used previously to study the cellular accumulation of LAT1-utilizing compounds (23-26). As seen in **Figure 2**, the expression levels of LAT1 and 4F2hc were highest in UT-SCC-42B cells (0.56 ± 0.19 fmol/μg protein and 1.69 ± 0.59 fmol/μg protein, respectively) and lowest in U-87MG cells (0.007 ± 0.003 fmol/μg protein and 0.0015 ± 0.0003 fmol/μg protein, respectively). Interestingly, MCF-7 and UT-SCC-28 cells also had relatively low LAT1 expression (0.028 ± 0.002 fmol/μg protein and 0.012 ± 0.006 fmol/μg protein, respectively). Moreover, in U-87MG and MCF-7 cells, the amount of 4F2hc was ca. one-fifth that of LAT1, while in UT-SCC-28 and UT-SCC-42B cells the amount was 3-times higher. This may imply that the latter cells also express other heterodimeric transporters, which require 4F2hc to be functional on the plasma membrane, such as L-type amino acid transporter 2, LAT2 (*SLC7A8*) and/or cystine-glutamate antiporter, xCT (*SLC7A11*), that were not studied herein.

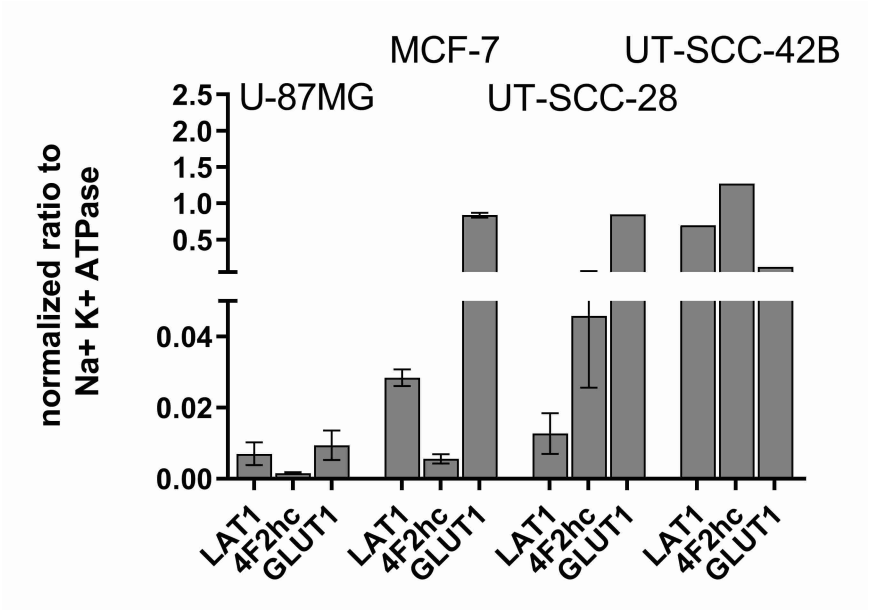

Figure 2. Protein expression levels of L-type amino acid transporter 1 (LAT1) light chain, CD98 heavy chain (4F2hc), and glucose transporter 1 (GLUT1) normalized to the expression of sodium-potassium adenosine triphosphatase (Na^+/K^+-ATPase) in different cancer cell lines; human glioma U-87MG, human breast cancer (MCF-7), and squamous cell carcinomas UT-SCC-28 and UT-SCC-42B. The protein levels were analyzed from the plasma membranes and normalized to the total amount of protein in the plasma membrane prior to Na^+/K^+-ATPase normalization. The results are expressed as mean ± SD (n = 3 biological replicates).

To confirm that LAT1 was also functional on the plasma membrane of selected cell types, concentration-dependent uptake of a LAT1 probe substrate [^{14}C]-L-leucine was carried out (**Table 2**). According to the Michaelis-Menten kinetics, the highest accumulation of [^{14}C]-L-Leu was achieved with UT-SCC-42B (V_{max} 16.26 ± 0.36 nmol/min/mg protein) followed by UT-SCC-28 (V_{max} 7.66 ± 0.34 nmol/min/mg protein) and U-87MG (V_{max} 0.85 ± 0.05 nmol/min/mg protein), which also correlated with the expression levels of LAT1 in these cells (**Figure 2**). The cellular accumulation of [^{14}C]-L-Leu was relatively fast, so the concentration-dependent uptake curve reached saturation at relatively high concentrations and therefore, the K_m values were relatively high (110-200 μM). These followed the order of the accumulation extent: U-87MG < UT-SCC-28 < UT-SCC-42B (**Table 2**). The cellular uptake of 0.38 and 0.76 μM of [^{14}C]-L-Leu was also inhibited with a specific LAT1-inhibitor (100 μM) (33), confirming that the uptake of the probe substrate was LAT1-mediated (**Figure 3**).

Table 2. Michaelis-Menten kinetic parameters (V_{max} and K_m) of [^{14}C]-L-Leu uptake into human squamous cell carcinoma, UT-SCC-28, UT-SCC-42B cells, and human glioma, U-87MG cells.

Cell line	V_{max} (nmol/min/mg protein)	K_m (μM)
U-87MG	0.85 ± 0.05	110.0 ± 15.9
UT-SCC-28	7.66 ± 0.34	200.3 ± 18.7
UT-SCC-42B	16.26 ± 0.36	299.6 ± 12.5

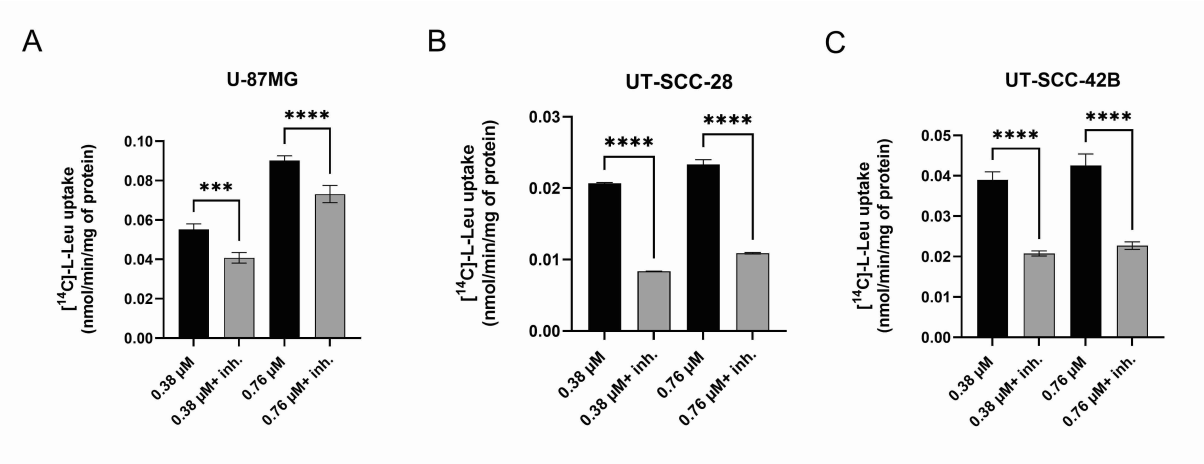

Figure 3. The cellular uptake of [^{14}C]-L-Leu (0.38 μM and 0.76 μM) in the absence (black bars) and presence of selective LAT1-inhibitor (100 μM; grey bars) into human glioma U-87MG, and squamous cell carcinomas UT-SCC-28 and UT-SCC-42B. The data are expressed as mean ± SD (n = 3) and an asterisk denotes a statistically significant difference between the groups (*** $P < 0.001$, **** $P < 0.0001$, one-way ANOVA, followed by Tukey's multiple comparison test).

*3.3 LAT1-Mediated Cellular Uptake of TMZ-AA **6** Into Human Glioma Cells*

The cellular uptake efficiency of TMZ and TMZ-AA **6** was evaluated with the selected cell lines expressing functional LAT1 (human glioma U-87MG, human squamous cell carcinoma UT-SCC-28 and UT-SCC-42B cells; **Figure 4**). Curiously, the uptake of TMZ and TMZ-AA **6** were more or less equal in U-87MG and UT-SCC-28 cells (V_{max} 32.3 ± 17.2 and 27.4 ± 2.9 pmol/min/mg protein, respectively, in U-87MG cells; and V_{max} 172.0 ± 97.4 and 204.3 ± 104.7 pmol/min/mg protein, respectively, in UT-SCC-28 cells). Notably, at higher concentrations, the uptake of TMZ into U-87MG cells was even higher than the uptake of TMZ-AA **6**. In contrast, in UT-SCC-42B cells, the uptake of TMZ-AA **6** was over 20-times greater compared with TMZ itself (V_{max} 591.6 ± 34.8 and 27.4 ± 6.3 pmol/min/mg protein, respectively). This high cellular uptake rate of TMZ-AA **6** into UT-SCC-42B cells is consistent with these expressing the highest level of functional LAT1 on the plasma membrane. In UT-SCC-42B cells, the K_m value of TMZ-AA **6** was lower (24.9 ± 4.9 μM) and closer to the values seen with other natural and non-natural substrates of LAT1 (< 50 μM), while in U-87MG and UT-SCC-28 cells, the K_m values of TMZ-AA **6** (74.4 ± 18.6 and 570 ± 371 μM, respectively) were closer to the K_m values of [^{14}C]-L-Leu determined in this study. Moreover, as seen in **Figure 5**, the specific LAT1-inhibitor (33), inhibited the uptake of TMZ-AA more effectively in UT-SCC-42B and U-87MG cells than in UT-SCC-28 cells, implying that the cellular uptake into the former two cell lines was mainly LAT1-mediated, while the transport into the latter one was more likely mediated by other transport mechanisms. The very high K_m value (570 ± 371 μM) indicates a low-affinity transport mechanism other than LAT1. Furthermore, TMZ itself was able to utilize at least two distinct transport mechanisms as seen in **Figure 5** (**A**, **C**, **E**); the higher concentrations were not following the uptake rate profile of the lower concentrations. However, this observation needs to be confirmed with more data points, which was not the scope of the present study focusing on the properties of the new derivative TMZ-AA **6**.

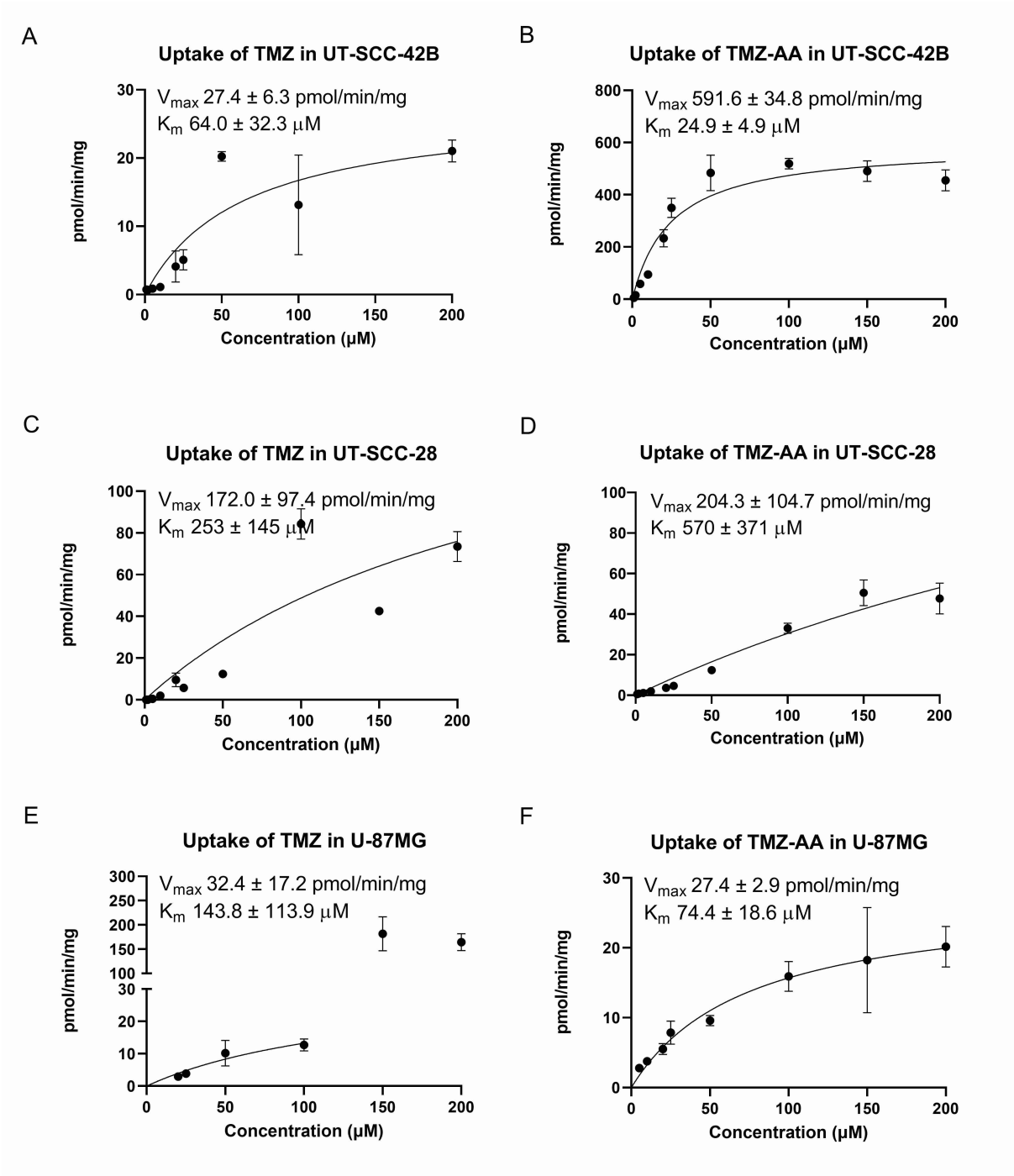

Figure 4. The cellular uptake of temozolomide (TMZ) and its LAT1-utilizing amino acid derivative TMZ-AA **6** into human squamous cell carcinoma, UT-SCC-42B cells (**A**-**B**), UT-SCC-28 cells (**C**-**D**), and glioma U-87MG cells (**E**-**F**). The data are presented as mean ± SD (n = 3).

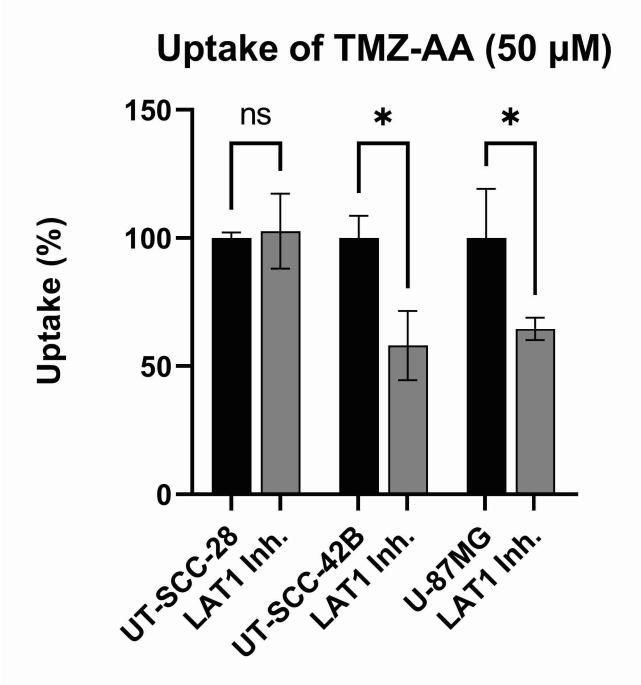

Figure 5. The cellular uptake of TMZ-AA **6** (50 µM) into human squamous cell carcinoma, UT-SCC-28, UT-SCC-42B, and glioma U-87MG cells in the absence (black bars) and the presence of selective LAT1-inhibitor (100 µM; grey bars). The data are presented as mean ± SD (n = 3) and an asterisk denotes a statistically significant difference between the groups (* $P < 0.01$, one-way ANOVA, followed by Tukey's multiple comparison test).

3.4 Antiproliferative Effects of TMZ-AA ***6*** *Used in Mono- and Combination Therapies*

When incubating the selected cancer cells with TMZ or TMZ-AA **6** (5-200 μM) for 72 h hours (the incubation media was changed and replaced with a fresh one containing the studied compounds every 24 h), modest effects on cell viability were detected only at the highest concentrations studied (**Figure S5**). All cell lines were insensitive to TMZ, consistent with MGMT proficiency, with the three cell lines showing modest (approx. 50%) reductions in viability at 200 μM (38, 39). For TMZ-AA **6**, the glioma cell line remained resistant even at 200 μM, whilst in the carcinoma cell lines, potency at 200 μM appeared independent of LAT1 transport despite the 20-fold greater uptake established in UT-SCC-42B cells.

Even though U-87MG cells are usually regarded as MGMT-negative and so TMZ-sensitive, they have been reported to gain adapted TMZ resistance (38). Therefore, the role of resistance mechanisms in the viability studies with TMZ and TMZ-AA **6** was explored using resistance mechanism inhibitors. First, the effects of TMZ and TMZ-AA **6** were studied in the presence of the MGMT-inhibitor *O*6-benzylguanine (BG). As expected, BG (100 μM) potentiated the cytotoxic effects of TMZ and TMZ-AA **6** even at the lowest imidazotetrazine concentrations (>> 5 μM), in all three cell types (**Figure 6**). Somewhat surprisingly, the control data for BG alone showed confounding cell viability loss at 100 μM in the U-87MG and UT-SCC-42B cells of about 60% (**Figure S6**). In U-87MG cells, the cell viability in both BG+TMZ and BG+TMZ-AA **6** combinations was reduced beyond the BG control values to 75-78% and 73-74%, respectively at all imidazotetrazine concentrations after 72 h, and no difference was seen between the two test compounds. This finding was interesting, since U-87MG cells are usually regarded as MGMT-negative cells, and increasing MGMT expression has been reported to be developed within several weeks of TMZ treatment (40). Therefore, it can be speculated that these cells may develop MGMT-resistance to TMZ-like alkylating compounds more rapidly than previously reported. Notably, the increased effects of the combination therapy on the cell viability were already evident after 24 h (41-52% reduction with TMZ+BG combination and 46-57% reduction with TMZ-AA+BG combination; **Figure S7**), thereby showing that MGMT-activity was already present during the first 24 h.

Similarly, in the LAT1-proficient UT-SCC-42B cells, the effect of BG alone was already significant (**Figure S6**; 61% reduction). Therefore, the combination treatment with TMZ and TMZ-AA **6**, showed only minor additional viability effects at higher concentrations (*e.g.*, at

200 μM; 87% and 85% reduction, respectively). In contrast, BG alone showed no decrease in UT-SCC-28 cell viability (**Figure S6**), but the combination of BG with TMZ or TMZ-AA **6** reduced the cell viability (**Figure 6**). However, TMZ+BG co-treatment was a little more effective at low concentrations (5 μM) in reducing the cell viability than TMZ-AA+BG co-treatment (76% vs. 53% reduction, respectively) after 72 h, while at higher concentrations (200 μM), the effects were almost equal for both compound combinations (84% vs. 83%).

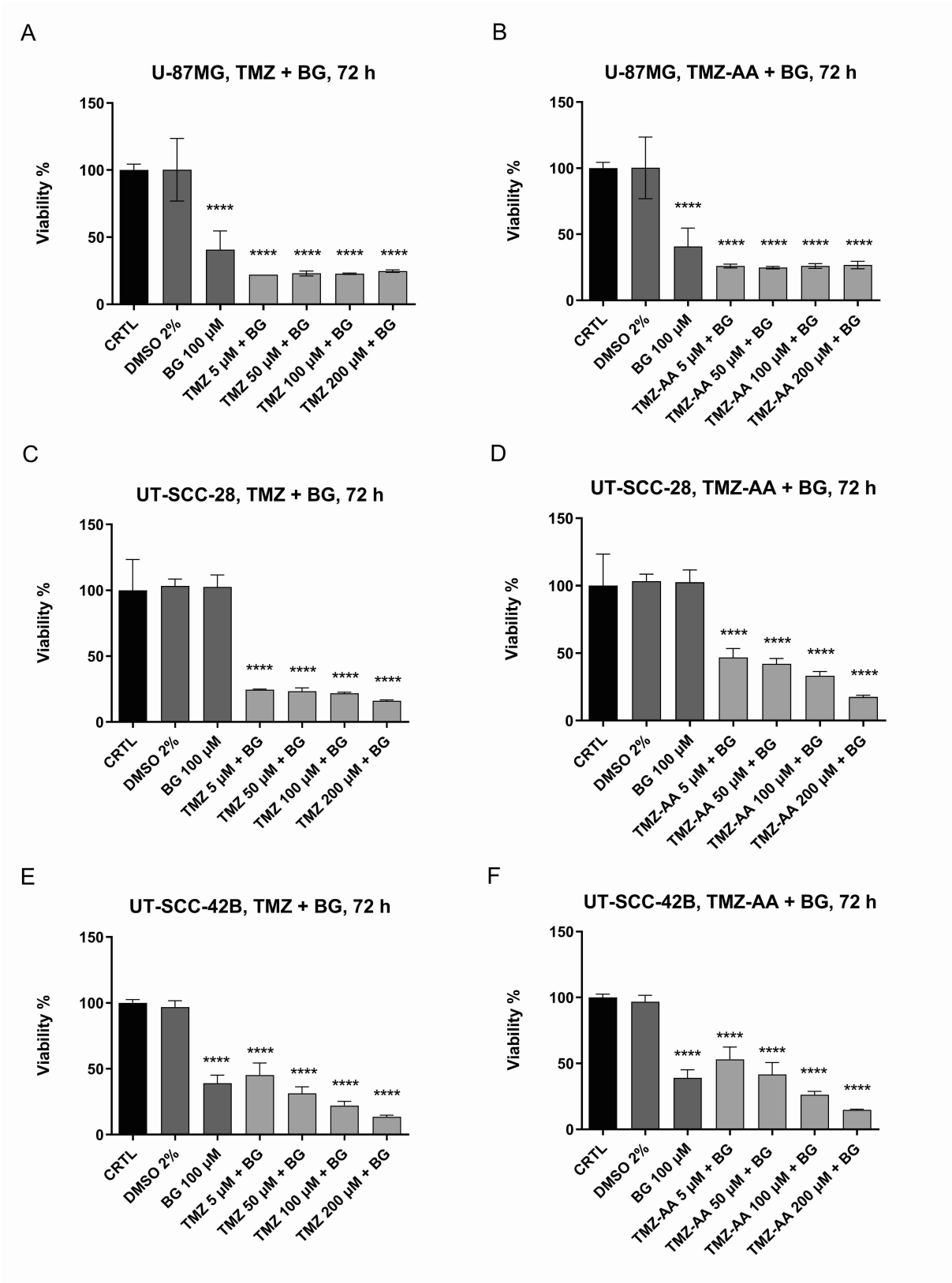

Figure 6. The cellular viability of human glioma U-87MG cells (**A**-**B**), human squamous cell carcinoma, UT-SCC-28 cells (**C**-**D**), and UT-SCC-42B cells (**E**-**F**), in the presence of TMZ (5-200 µM; **A**, **C**, **E**) or TMZ-AA **6** (5-200 µM; **B**, **D**, **F**) combined with *O*6-benzylguanine (BG; 100 µM) (light grey bars) after 72 h. The viability is compared with the untreated control cells

(black bars) and presented as percentages (%). Maximum amount of DMSO (2%) and BG alone (100 μM) were used as controls (dark grey bars). The data are presented as mean ± SD (n = 3-6) and an asterisk denotes a statistically significant difference between the groups **** $P < 0.0001$ one-way ANOVA, followed by Dunnett's multiple comparison test).

Since the effects were less marked at lower concentrations of imidazotetrazine co-treatments in UT-SCC-42B cells, we also sought to test a triple combination, adding a BER-inhibitor, methoxyamine (MX), to the treatment combination. The controls with MX alone (**Figure S6 A**, **C**, **E**) showed that there was no reduction in cell viability upto 100 μM in U-87MG and UT-SCC-28 cells, while UT-SCC-42B cells showed a concentration-dependent loss of viability above 50 μM, this being about 50% at 100 μM MX. Moreover, U-87MG cells treated with a two-component combination; TMZ or TMZ-AA **6** (5-200 μM) with MX (100 μM) were the most sensitive to the treatment, whilst the viability of UT-SCC28 and UT-SCC42B cells was reduced only at the highest TMZ or TMZ-AA concentrations (200 μM) (**Figure 7**). However, this was not due to the combination treatment, since TMZ and TMZ-AA **6** had the same level reduction effect already as single treatment. Therefore, it can be noted that in UT-SCC-42B cells, TMZ and TMZ-AA **6** were able to abolish the effects of MX on cell viability.

The effects of triple-combination were much greater than two-component combinations in all cell types and the increased cytotoxicity was evident at the lowest concentration tested (5 μM) reducing the cell viability by approximately 70% (**Figure 8**). Moreover, the effect of triple-combination was also greater than the single treatment MX or BG controls (**Figure S7**), indicating that the effects were synergistic and not arising from a single component of the treatment mixture. Notably, the effects of triple-combination with U-87MG glioma cells were so strong that the cell viability was reduced to ca. 30% after only 24 h incubation (**Figure S8**). A slightly lesser, concentration-dependent effect was seen with UT-SCC-28 and UT-SCC-42B cells; but once again there was no clear difference between TMZ-combinations and TMZ-AA-combinations. Therefore, it can be concluded that major improvements in TMZ-therapy are more likely to be achieved by increasing the intensity of DNA methylation rather than increasing the cell permeation.

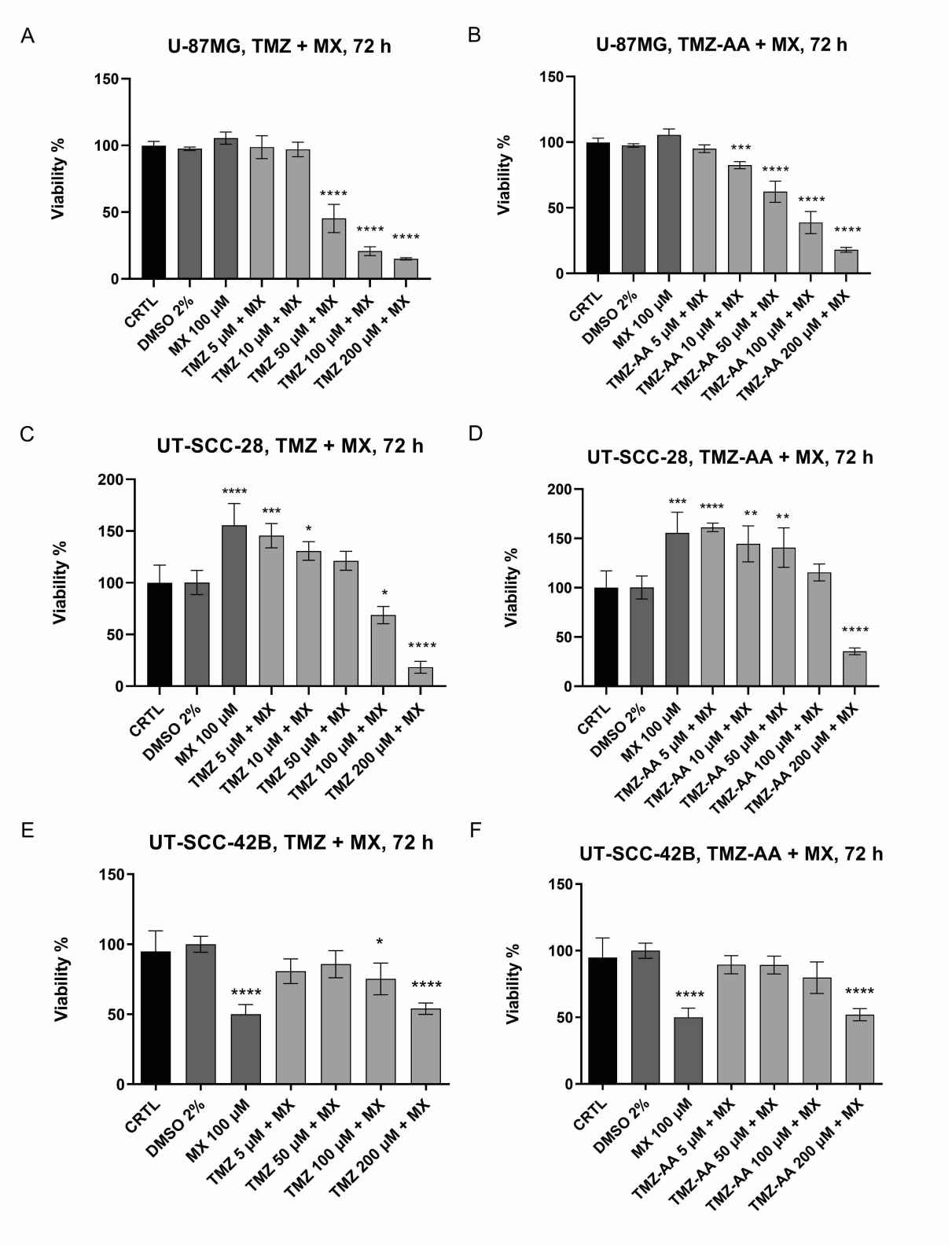

Figure 7. The cellular viability of human glioma U-87MG cells (**A**-**B**), human squamous cell carcinoma, UT-SCC-28 cells (**C**-**D**), and UT-SCC-42B cells (**E**-**F**), in the presence of TMZ (5-200 µM; **A**, **C**, **E**) or TMZ-AA **6** (5-200 µM; **B**, **D**, **F**) combined with methoxyamine (MX; 100 µM) (light grey bars) after 72 h. The viability is compared with the untreated control cells (black bars) and presented as percentages (%). Maximum amount of DMSO was used as a

negative control (dark grey bars). The data are presented as mean ± SD (n = 3-6) and an asterisk denotes a statistically significant difference between the groups * $P < 0.05$, ** $P < 0.01$, *** $P < 0.001$, **** $P < 0.0001$ one-way ANOVA, followed by Dunnett's multiple comparison test).

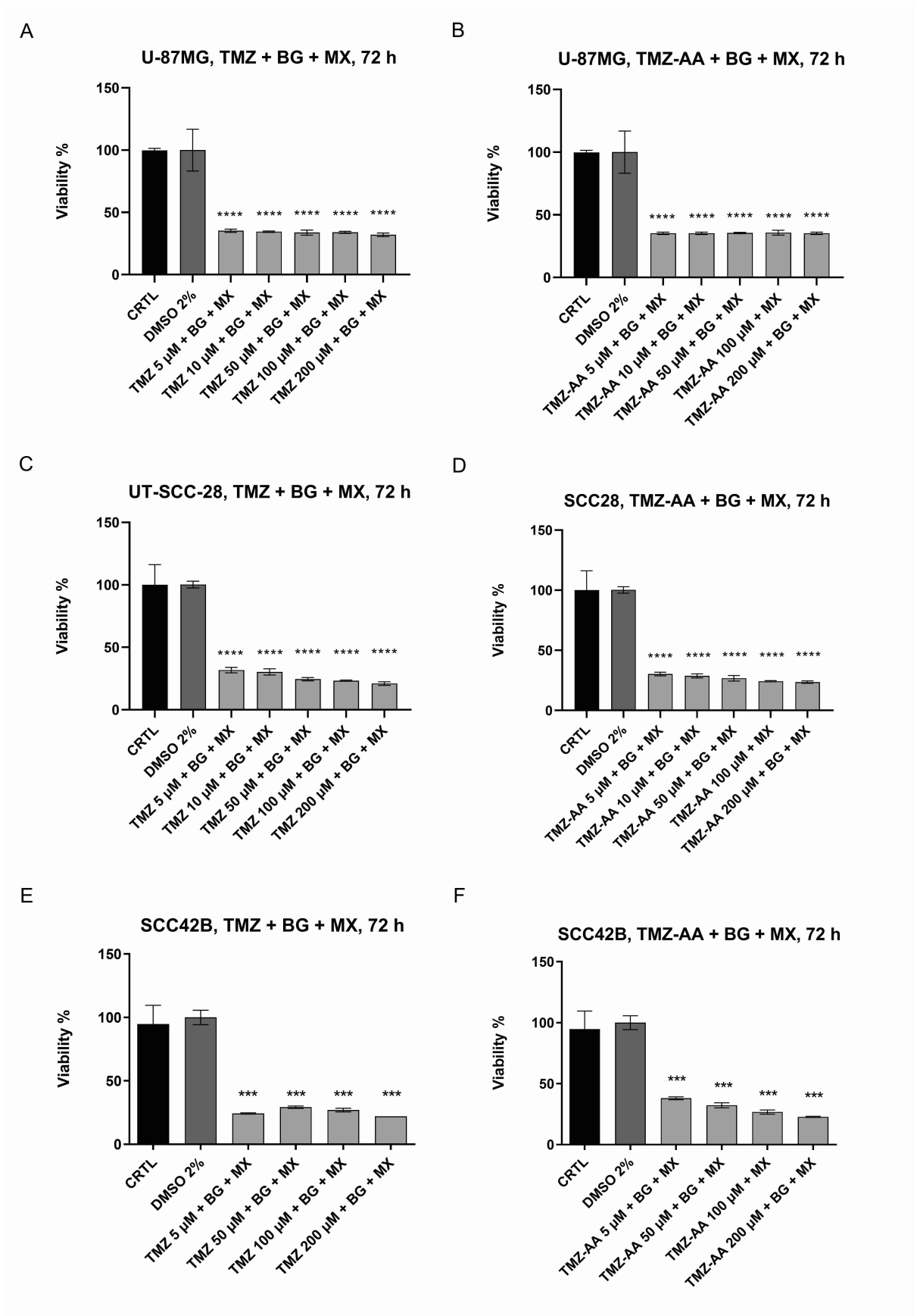

Figure 8. The cellular viability of human glioma U-87MG cells (**A**-**B**), human squamous cell carcinoma, UT-SCC-28 cells (**C**-**D**), and UT-SCC-42B cells (**E**-**F**), in the presence of TMZ (5-

200 μM; **A**, **C**, **E**) or TMZ-AA **6** (5-200 μM; **B**, **D**, **F**) and *O*6-benzylguanine and methoxyamine (BG + MX; 100 + 100 μM) (grey bars) after 72 h. The viability is compared with the untreated control cells (black bars) and presented as percentages (%). Maximum amount of DMSO (2%) was used as a negative control (dark grey bars). The data are presented as mean ± SD (n = 3-6) and an asterisk denotes a statistically significant difference between the groups **** $P < 0.0001$ one-way ANOVA, followed by Dunnett's multiple comparison test).

4 Discussion

Since its discovery in the 1980s and approval in the 1990s, the methylating agent TMZ has become the standard of care for the treatment of brain tumors, such as glioblastoma.(11) However, the short hydrolytic stability of TMZ ($t_{½}$ < 2 h) is speculated to be one of the key factors limiting its anti-cancer effectiveness (17). It is barely enough time for TMZ to reach the brain, penetrate its target sites, and release the active methyl diazonium ion in cancerous cells. Therefore, several TMZ derivatives have been prepared with the aim of increasing the hydrolytic stability at pH 7.4. It has been noticed that adding different substituents to the C8 (amide) position could be one option (18, 41). However, in the present study, attaching an amino acid residue to the C8-position did not increase the hydrolytic stability in a buffer solution at pH 7.4 and +37 °C (**Table 1**). Nevertheless, the improved anticancer effects have also been noticed to be related to the increased brain/plasma ratio rather than the hydrolytic stability (41). Moreover, not all reported C8-substituents result in increased brain permeation. Rai et al. noted that a β-carboline substituent also increases the tissue protein/lipid binding and thus, there was less free prodrug to release methyl diazonium ions at the tumor target site (41). It has also recently been reported that simple C8-ester derivatives of TMZ can improve the cytotoxic effects of TMZ, and simultaneously also reverse one of the TMZ resistance mechanisms via the down-regulation of MGMT (42). However, it is not clear whether this anti-resistance effect arises from the novel compound itself or from the fact that it is hydrolyzed not only chemically to release the methyl diazonium ion, but also enzymatically to release an alcoholic metabolite with a long hydrocarbon chain that may have also affect cells.

In the present study, TMZ was successfully converted into 8-phenylalanine conjugate TMZ-AA **6** (**Scheme 1**) that was studied as a LAT1-substrate. The new TMZ-AA **6** was shown to be an effective substrate for LAT1 in cells expressing a sufficient amount of LAT1, such as UT-SCC-42B cells (**Figure 2**). Moreover, the utilization of LAT1-mediated transport by TMZ-AA in these cells increased the delivery of the methylating agent compared with TMZ (**Figure 4-5**). However, the lower expression levels of LAT1, seen in U-87MG and UT-SCC-28 cells, were not sufficient to increase cellular uptake of TMZ-AA above the levels of TMZ. Furthermore, the increased delivery into UT-SCC-42B cells did not improve the cytotoxic effects of TMZ (**Figure S5**). Only by combining the alkylating agent with inhibitors of DNA repair (MGMT inhibitor *O*6-benzylguanine; BER inhibitor methoxyamine) in dual and triple agent co-treatments, was activity equivalent to TMZ achieved for TMZ-AA **6** (**Figures 6-8**).

Thus, this study indicates that the critical step of TMZ-like alkylating compounds to gain treatment success is to secure efficient DNA-alkylation by inhibiting the DNA-repairing resistance mechanisms rather than increasing the delivery *per se* of alkylating agents into the cells. However, since LAT1 is highly expressed at the BBB, utilizing the transporter (like LAT1), can be beneficial to improve the brain delivery of drugs (43, 44). Moreover, with LAT1 being overexpressed specifically in many cancer cells (21, 45), it can serve as a carrier for targeted drug delivery, which can ultimately improve efficacy selectively at the target cells and thus, decrease unwanted DNA methylation in healthy non-cancerous cells.

An effective design strategy to improve the anticancer activity of TMZ has been to circumvent both MGMT-and MMR-resistance mechanisms by replacing the simple methyl diazonium with other highly reactive ions, such as propargyl or aziridine-precursor diazonium ions that can elicit pharmacological activity from the major site of reaction of DNA, G-*N*7 rather than the minor sites, G-*O*6 and A-*N*3 (9, 46-48). Combining these compounds with C8-derivatization and specific transporter utilization to increase selectivity and efficiency of brain penetration and accumulation to tumor target cells, could yield effective brain tumor chemotherapy.

5 Conclusions

In conclusion, TMZ can be converted to a LAT1-utilizing derivative to improve its cellular uptake. However, attaching the amino acid moiety to the C8-position did not increase the chemical stability of the tetrazine ring. Moreover, the increased delivery did not improve the cytotoxic properties of TMZ. Instead, this study concludes that the TMZ-related chemoresistance can only be overcome by inhibiting the DNA repair systems, including MGMT, MMR, and BER, with combination therapies or by developing alkylating compounds that can liberate alternative, major site-attacking alkylating species that are not substrates for these DNA repair systems.

Acknowledgments

The authors would like to thank Ms. Tiina Koivunen for her technical assistance with the bioconversion and uptake studies and Professor Reidar Grenman at the Department of Otorhinolaryngology, University of Turku and Turku University Hospital for donating the UT-SCC cell lines.

Conflict of Interest

The authors declare that the research was conducted in the absence of any commercial or financial relationships that could be construed as a potential conflict of interest.

Funding

The study was financially supported by the Academy of Finland (grants 294227, 294229, 307057, 311939), and Yorkshire Cancer Research (grant number B210).

References

1. Bergo E, Lombardi G, Pambuku A, Della Puppa A, Bellu L, D'Avella D, et al. Cognitive rehabilitation in patients with gliomas and other brain tumors: state of the art. Biomed Res Int. 2016;2016:3041824.vol(part)??

2. Wang Y, Wang Z, Hua C, Xu Y, Li Y, Zhao G. Primary malignant brain tumors following systemic malignancies: a population-based analysis. Neuroepidemiology. 2022. vol(part)&pp?

3. Aizer AA, Lamba N, Ahluwalia MS, Aldape K, Boire A, Brastianos PK, et al. Brain metastases: A Society for Neuro-Oncology (SNO) consensus review on current management and future directions. Neuro Oncol. 2022;24(10):1613-46.

4. Senger D, Cairncross JG, Forsyth PA. Long-term survivors of glioblastoma: statistical aberration or important unrecognized molecular subtype? Cancer J. 2003;9(3):214-21.

5. Pardridge WM. A historical review of brain drug delivery. Pharmaceutics. 2022;14(6).pp?

6. Partridge B, Eardley A, Morales BE, Campelo SN, Lorenzo MF, Mehta JN, et al. Advancements in drug delivery methods for the treatment of brain disease. Front Vet Sci. 2022;9:1039745.(part?)

7. Upton DH, Ung C, George SM, Tsoli M, Kavallaris M, Ziegler DS. Challenges and opportunities to penetrate the blood-brain barrier for brain cancer therapy. Theranostics. 2022;12(10):4734-52.

8. Mitusova K, Peltek OO, Karpov TE, Muslimov AR, Zyuzin MV, Timin AS. Overcoming the blood-brain barrier for the therapy of malignant brain tumor: current status and prospects of drug delivery approaches. J Nanobiotechnol. 2022;20(1):412.page range?

9. Ramirez YP, Weatherbee JL, Wheelhouse RT, Ross AH. Glioblastoma multiforme therapy and mechanisms of resistance. Pharmaceuticals (Basel). 2013;6(12):1475-506.

10. Moody CL, Wheelhouse RT. The medicinal chemistry of imidazotetrazine prodrugs. Pharmaceuticals (Basel). 2014;7(7):797-838.

11. Stevens MFG, Wheelhouse RT. Antitumour imidazotetrazines: past, present… and future? RSC Chem Biol. 2023;4(10):736-741.

12. Wheelhouse RT, Stevens MFG. Decomposition of the antitumour drug temozolomide in deuteriated phosphate buffer: methyl group transfer is accompanied by deuterium exchange. J Chem Soc, Chem Commun. 1993(15):1177-8.

13. Zhang J, Stevens MF, Bradshaw TD. Temozolomide: mechanisms of action, repair and resistance. Curr Mol Pharmacol. 2012;5(1):102-14.

14. Woo P, Li Y, Chan A, Ng S, Loong H, Chan D, et al. A multifaceted review of temozolomide resistance mechanisms in glioblastoma beyond O-6-methylguanine-DNA methyltransferase. Glioma. 2019;2(2):68-82.

15. Tomar MS, Kumar A, Srivastava C, Shrivastava A. Elucidating the mechanisms of Temozolomide resistance in gliomas and the strategies to overcome the resistance. Biochim Biophys Acta Rev Cancer. 2021;1876(2):188616.page range?

16. Goellner EM, Grimme B, Brown AR, Lin YC, Wang XH, Sugrue KF, et al. Overcoming temozolomide resistance in glioblastoma via dual inhibition of NAD+ biosynthesis and base excision repair. Cancer Res. 2011;71(6):2308-17.

17. Jatyan R, Singh P, Sahel DK, Karthik YG, Mittal A, Chitkara D. Polymeric and small molecule-conjugates of temozolomide as improved therapeutic agents for glioblastoma multiforme. J Control Release. 2022;350:494-513.(part)

18. Svec RL, Furiassi L, Skibinski CG, Fan TM, Riggins GJ, Hergenrother PJ. Tunable Stability of Imidazotetrazines Leads to a Potent Compound for Glioblastoma. ACS Chem Biol. 2018;13(11):3206-16.

19. Janjua TI, Cao Y, Ahmed-Cox A, Raza A, Moniruzzaman M, Akhter DT, et al. Efficient delivery of Temozolomide using ultrasmall large-pore silica nanoparticles for glioblastoma. J Control Release. 2023;357:161-74.(part?)

20. Yasaswi PS, Shetty K, Yadav KS. Temozolomide nano enabled medicine: promises made by the nanocarriers in glioblastoma therapy. J Control Release. 2021;336:549-71. (part?)

21. Hafliger P, Charles RP. The L-Type Amino Acid Transporter LAT1-An Emerging Target in Cancer. Int J Mol Sci. 2019;20(10).pages?

22. Zhang C, Xu J, Xue S, Ye J. Prognostic Value of L-Type Amino Acid Transporter 1 (LAT1) in Various Cancers: A Meta-Analysis. Mol Diagn Ther. 2020;24(5):523-36.

23. Karkkainen J, Gynther M, Kokkola T, Petsalo A, Auriola S, Lahtela-Kakkonen M, et al. Structural properties for selective and efficient l-type amino acid transporter 1 (LAT1) mediated cellular uptake. Int J Pharm. 2018;544(1):91-99.

24. Kärkkäinen J, Laitinen T, Markowicz-Piasecka M, Montaser A, Lehtonen M, Rautio J, et al. Molecular characteristics supporting l-Type amino acid transporter 1 (LAT1)-mediated translocation. Bioorg Chem. 2021;112:104921.

25. Thiele NA, Karkkainen J, Sloan KB, Rautio J, Huttunen KM. Secondary carbamate linker can facilitate the sustained release of dopamine from brain-targeted prodrug. Bioorg Med Chem Lett. 2018;28(17):2856-60.

26. Huttunen J, Gynther M, Vellonen KS, Huttunen KM. L-Type amino acid transporter 1 (LAT1)-utilizing prodrugs are carrier-selective despite having low affinity for organic anion transporting polypeptides (OATPs). Int J Pharm. 2019;571:118714. (part?)

27. Uchida Y, Tachikawa M, Obuchi W, Hoshi Y, Tomioka Y, Ohtsuki S, et al. A study protocol for quantitative targeted absolute proteomics (QTAP) by LC-MS/MS: application for inter-strain differences in protein expression levels of transporters, receptors, claudin-5, and marker proteins at the blood-brain barrier in ddY, FVB, and C57BL/6J mice. Fluids Barriers CNS. 2013;10(1):21.

28. Huttunen J, Agami M, Tampio J, Montaser AB, Huttunen KM. Comparison of Experimental Strategies to Study l-Type Amino Acid Transporter 1 (LAT1) Utilization by Ligands. Molecules. 2021;27(1).pages?

29. Montaser AB, Järvinen J, Löffler S, Huttunen J, Auriola S, Lehtonen M, et al. (missing authors??) L-Type amino acid transporter 1 enables the efficient brain delivery of small-sized prodrug across the blood-brain barrier and into human and mouse brain parenchymal cells. ACS Chem Neurosci. 2020;11(24):4301-15.

30. Markowicz-Piasecka M, Huttunen J, Montaser A, Adla SK, Auriola S, Lehtonen M, et al.(missing authors?) Ganciclovir and its hemocompatible more lipophilic derivative can enhance the apoptotic effects of methotrexate by inhibiting breast cancer resistance protein (BCRP). Int J Mol Sci. 2021;22(14).pages?

31. Uchida Y, Zhang Z, Tachikawa M, Terasaki T. Quantitative targeted absolute proteomics of rat blood-cerebrospinal fluid barrier transporters: comparison with a human specimen. J Neurochem. 2015;134(6):1104-15.

32. Uchida Y, Yagi Y, Takao M, Tano M, Umetsu M, Hirano S, et al. (missing authors?) Comparison of absolute protein abundances of transporters and receptors among blood-brain barriers at different cerebral regions and the blood-spinal cord barrier in humans and rats. Mol Pharm. 2020;17(6):2006-20.

33. Huttunen KM, Gynther M, Huttunen J, Puris E, Spicer JA, Denny WA. A Selective and Slowly Reversible Inhibitor of l-Type Amino Acid Transporter 1 (LAT1) Potentiates Antiproliferative Drug Efficacy in Cancer Cells. J Med Chem. 2016;59(12):5740-51.

34. Peura L, Malmioja K, Laine K, Leppanen J, Gynther M, Isotalo A, et al. (missing authors) Large amino acid transporter 1 (LAT1) prodrugs of valproic acid: new prodrug design ideas for central nervous system delivery. Mol Pharm. 2011;8(5):1857-66.

35. Puris E, Gynther M, Huttunen J, Petsalo A, Huttunen KM. L-Type amino acid transporter 1 utilizing prodrugs: how to achieve effective brain delivery and low systemic exposure of drugs. J Control Release. 2017;261:93-104.(part?)

36. Peura L, Malmioja K, Huttunen K, Leppanen J, Hamalainen M, Forsberg MM, et al. (missing authors?) Design, synthesis and brain uptake of LAT1-targeted amino acid prodrugs of dopamine. Pharm Res. 2013;30(10):2523-37.

37. Horspool KR, Stevens MF, Newton CG, Lunt E, Walsh RJ, Pedgrift BL, et al. Antitumor imidazotetrazines. 20. Preparation of the 8-acid derivative of mitozolomide and its utility in the preparation of active antitumor agents. J Med Chem. 1990;33(5):1393-9.

38. Lee SY. Temozolomide resistance in glioblastoma multiforme. Genes Dis. 2016;3(3):198-210.

39. Poon MTC, Bruce M, Simpson JE, Hannan CJ, Brennan PM. Temozolomide sensitivity of malignant glioma cell lines - a systematic review assessing consistencies between in vitro studies. BMC Cancer. 2021;21(1):1240.

40. Kohsaka S, Wang L, Yachi K, Mahabir R, Narita T, Itoh T, et al. STAT3 inhibition overcomes temozolomide resistance in glioblastoma by downregulating MGMT expression. Mol Cancer Ther. 2012;11(6):1289-99.

41. Rai R, Banerjee M, Wong DH, McCullagh E, Gupta A, Tripathi S, et al. Temozolomide analogs with improved brain/plasma ratios - Exploring the possibility of enhancing the therapeutic index of temozolomide. Bioorg Med Chem Lett. 2016;26(20):5103-9.

42. Yu Y, Wang L, Han J, Wang A, Chu L, Xi X, et al. Synthesis and Characterization of a Series of Temozolomide Esters and Its Anti-glioma Study. J Pharm Sci. 2021;110(10):3431-8.

43. Boado RJ, Li JY, Nagaya M, Zhang C, Pardridge WM. Selective expression of the large neutral amino acid transporter at the blood-brain barrier. Proc Natl Acad Sci USA. 1999;96(21):12079-84.

44. Prasad PD, Wang H, Huang W, Kekuda R, Rajan DP, Leibach FH, et al. Human LAT1, a subunit of system L amino acid transporter: molecular cloning and transport function. Biochem Biophys Res Commun. 1999;255(2):283-8.

45. Yanagida O, Kanai Y, Chairoungdua A, Kim DK, Segawa H, Nii T, et al. Human L-type amino acid transporter 1 (LAT1): characterization of function and expression in tumor cell lines. Biochim Biophys Acta. 2001;1514(2):291-302.

46. Ramirez YP, Mladek AC, Phillips RM, Gynther M, Rautio J, Ross AH, (missing authors?!!!!!!!!!!)et al. Evaluation of novel imidazotetrazine analogues designed to overcome temozolomide resistance and glioblastoma regrowth. Mol Cancer Ther. 2015;14(1):111-119.

47. Cousin D, Zhang J, Hummersone MG, Matthews CS, Frigerio M, Bradshaw TD, et al. (missing authors?) Antitumor imidazo[5,1-d]-1,2,3,5-tetrazines: compounds modified at the 3-position overcome resistance in human glioblastoma cell lines. MedChemComm. 2016;7(12):2332-43.

48. Pletsas D, Garelnabi EAE, Li L, Phillips RM, Wheelhouse RT. Synthesis and quantitative structure–activity relationship of imidazotetrazine prodrugs with activity independent of O6-methylguanine-DNA-methyltransferase, DNA mismatch repair, and p53. J. Med. Chem. 2013;56(17):7120-32.